

AD _____

Award Number: DAMD17-01-1-0558

TITLE: Monitoring Therapeutic Response of Metastatic Breast
Lesions Using Magnetic Resonance Imaging of Water
Self-Diffusion Coefficients

PRINCIPAL INVESTIGATOR: Douglas J. Ballon, Ph.D.

CONTRACTING ORGANIZATION: Sloan-Kettering Institute
for Cancer Research
New York, New York 10021

REPORT DATE: October 2003

TYPE OF REPORT: Final

PREPARED FOR: U.S. Army Medical Research and Materiel Command
Fort Detrick, Maryland 21702-5012

DISTRIBUTION STATEMENT: Approved for Public Release;
Distribution Unlimited

The views, opinions and/or findings contained in this report are those of the author(s) and should not be construed as an official Department of the Army position, policy or decision unless so designated by other documentation.

20040329 027

REPORT DOCUMENTATION PAGEForm Approved
OMB No. 074-0188

Public reporting burden for this collection of information is estimated to average 1 hour per response, including the time for reviewing instructions, searching existing data sources, gathering and maintaining the data needed, and completing and reviewing this collection of information. Send comments regarding this burden estimate or any other aspect of this collection of information, including suggestions for reducing this burden to Washington Headquarters Services, Directorate for Information Operations and Reports, 1215 Jefferson Davis Highway, Suite 1204, Arlington, VA 22202-4302, and to the Office of Management and Budget, Paperwork Reduction Project (0704-0188), Washington, DC 20503

1. AGENCY USE ONLY (Leave blank)		2. REPORT DATE October 2003	3. REPORT TYPE AND DATES COVERED Final (15 Sep 01-14 Sep 03)	
4. TITLE AND SUBTITLE Monitoring Therapeutic Response of Metastatic Breast Lesions Using Magnetic Resonance Imaging of Water Self-Diffusion Coefficients			5. FUNDING NUMBERS DAMD17-01-1-0558	
6. AUTHOR(S) Douglas J. Ballon, Ph.D.				
7. PERFORMING ORGANIZATION NAME(S) AND ADDRESS(ES) Sloan-Kettering Institute for Cancer Research New York, New York 10021 E-Mail: quirki@mskcc.org			8. PERFORMING ORGANIZATION REPORT NUMBER	
9. SPONSORING / MONITORING AGENCY NAME(S) AND ADDRESS(ES) U.S. Army Medical Research and Materiel Command Fort Detrick, Maryland 21702-5012			10. SPONSORING / MONITORING AGENCY REPORT NUMBER	
11. SUPPLEMENTARY NOTES				
12a. DISTRIBUTION / AVAILABILITY STATEMENT Approved for Public Release; Distribution Unlimited				12b. DISTRIBUTION CODE
13. ABSTRACT (Maximum 200 Words) <p>A new magnetic resonance imaging technique has been developed that is designed to detect and monitor metastatic breast lesions in bone marrow and other organs. Specifically, a diffusion sensitive echo planar magnetic resonance pulse sequence has been developed for both 1.5 Tesla and 3.0 Tesla whole-body imaging systems along with image processing techniques to facilitate whole-body screening for breast metastases. The acquisition sequence allows for multi-shot, multi-excitation imaging at multiple diffusion weighting values and is also compatible with phased array resonator use. Three-dimensional image reconstruction includes a paradigm for matching slabs of images obtained at multiple anatomical stations to yield a single field-of-view for rapid assessment of metastatic activity in subsequent clinical studies. Image display makes use of a pseudo-three-dimensional rotating presentation of maximum intensity projections through the three-dimensional dataset. In addition, the method is amenable to the measurement of coefficients of water-self diffusion on a voxel-by-voxel or region of interest basis anywhere in the body. This imaging technique requires no introduced contrast agents and can be completed in less than 20 minutes on conventional magnetic resonance scanners.</p>				
14. SUBJECT TERMS Magnetic resonance, diffusion imaging				15. NUMBER OF PAGES 28
				16. PRICE CODE
17. SECURITY CLASSIFICATION OF REPORT Unclassified	18. SECURITY CLASSIFICATION OF THIS PAGE Unclassified	19. SECURITY CLASSIFICATION OF ABSTRACT Unclassified	20. LIMITATION OF ABSTRACT Unlimited	

NSN 7540-01-280-5500

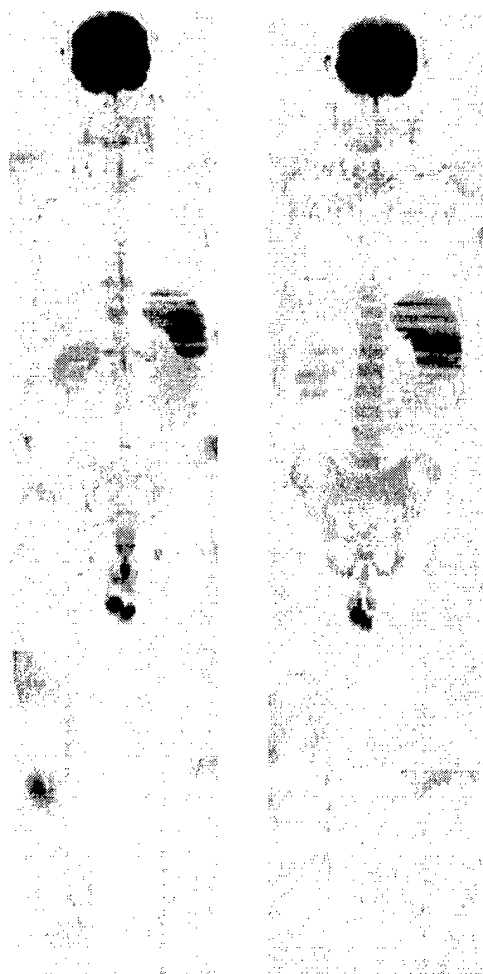
Standard Form 298 (Rev. 2-89)
Prescribed by ANSI Std. Z39-18
298-102

Table of Contents

Cover.....	1
SF 298.....	2
Introduction.....	4
Body.....	4
Key Research Accomplishments.....	5
Reportable Outcomes.....	6
Conclusions.....	6
References.....	6
Appendices/Bibliography.....	7
Personnel.....	7

Introduction:

During the period of the project a rapid non-invasive whole-body technique to monitor the response of metastatic breast lesions during therapy was developed using magnetic resonance imaging (MRI). Detection of metastatic lesions is one of the most important prognostic factors in breast cancer and as a consequence is critically important for disease staging and subsequent management (1). The proposed technique is based upon the use of echo planar magnetic resonance imaging combined with a method which renders the image contrast dependent upon the coefficient of self-diffusion of water. The total scan time for a single image was approximately 0.1 seconds, making the technique robust with respect to motion artifacts. For complete coverage from a field-of-view equal to 36 cm X 36 cm X 18 cm the scan times were approximately one minute. In a single scanning session data was acquired from six to eight stations simulating a whole-body study, for a total scan time of approximately thirty minutes including set-up time. This grant was awarded for technical development aspects of the overall project. The clinical applications presented below as examples were funded under a separate grant (NIH/NIBIB E002070).



Body:

Both 1.5 Tesla and 3.0 Tesla magnetic resonance systems (GE Medical Systems) were used for the work. In order to carry out tests of the methods a set of water-agarose/lipid-lecithin calibration phantoms were developed to mimic tissue composition in bone marrow. The pulse sequence employed spatial-spectral excitation (2,3) and multi-shot covering of k-space to limit image distortion, as well as multi-excitation acquisitions to improve the signal-to-noise ratio. We also investigated the use of shorter, stronger diffusion gradient pulses (up to 5 G/cm) than are typical (2.2 G/cm) on the scanners.

Image post-processing included a vendor-supplied fast fourier transform and distortion correction

Figure 1 - Maximum intensity projections of diffusion-weighted images from a bone marrow donor receiving G-CSF for marrow mobilization: A) pre G-CSF, B) post G-CSF.

for non-linearity in the magnetic field gradients. The diffusion images obtained along each spatial axis for each slice were combined according to

$$I(x,y) = [I_x(x,y)I_y(x,y)I_z(x,y)]^{1/3} = I_0(x,y)e^{-b\text{Tr}D^*} \quad [1]$$

where $I_j(x,y)$ represents the image intensity at a point (x,y) obtained with the diffusion gradients applied along the j th axis. The b -value is defined according to the Stejskal-Tanner relation and $\text{Tr}D^*$ represents the trace of the apparent diffusion coefficient tensor D^* (4). The trace images for all slices in all data blocks were stored in a three-dimensional array using the Interactive Data Language (IDL, Kodak). An inverse grayscale intensity scale was typically applied to the datasets for visual interpretation. Three-dimensional datasets were generated from the two-dimensional images, and were capable of display along any axis or alternatively displayed in a rotating format with the axis of rotation along the superior-inferior direction in the magnet frame of reference.



Figure 1 is presented to demonstrate a whole body application of the technique. In Figure 1(a) the data are from a normal volunteer bone marrow donor prior to receiving a cytokine for stem cell mobilization and subsequent bone marrow collection. Signal from the bone marrow is nearly absent. The data from Figure 1(b) were acquired five days later on the day of marrow harvest after administration of granulocyte-colony stimulating factor (G-CSF). A marked increase in bone marrow signal is observed in the axial skeleton, reflecting the stimulation of the bone marrow.

The results of imaging studies in a patient with stage IV breast cancer are presented in Figure 2. A whole-body image is presented from a study of a 68 year-old woman with stage IV disease exhibiting diffuse metastases in both the left and right femur.

Key Research Accomplishments:

- Development of quantitative water-agarose/lipid-lecithin calibration phantoms with matched T_1 and T_2 relaxation times to approximate bone marrow composition.

Figure 2 – Whole-body image of a 68-year old female with metastatic breast cancer. Bone marrow involvement is evident in the pelvis and in both legs.

- Development of the diffusion-weighted magnetic resonance pulse sequence allowing multi-shot, multi-excitation imaging at multiple diffusion weighting values.
- Development of post-processing software to produce three-dimensional whole-body datasets.

Reportable Outcomes:

1. Submitted manuscript on the development of calibration phantoms.
2. Abstract of International Society of Magnetic Resonance in Medicine 11th Annual Scientific Meeting Proceedings on applications of the method in patients (funded separately through NIH/NIBIB E002070).

Conclusions:

The rapid whole-body magnetic resonance imaging technique developed under the sponsorship of the USAMRMC will facilitate the investigation of the efficacy of therapeutic agents in metastatic breast cancer. The method is fast, robust with respect to patient motion, does not require introduced contrast agents, and can be implemented on clinical magnetic resonance systems currently in use.

References:

1. Harris JR, Morrow M, and Bonnadonna G, "Cancer of the Breast" in Cancer, Principles and Practice of Oncology, Devita VT, Hellman S, and Rosenberg SA eds. JB Lippincott Co., Philadelphia, 1993, Chapter 40.
2. Pauly J, Spielman D, and Macovski A. Echo-Planar Spin-Echo and Inversion Pulses, *Magnetic Resonance in Medicine*, 1993; **29**, 776-782.
3. Schick F, Forster J, Machann J, Kuntz R, and Claussen CD. Improved Clinical Echo-Planar MRI Using Spatial-Spectral Excitation, *J. of Magn. Res. Imag.*, 1998; **8**, 960-967.
4. Stejskal EO and Tanner JE. Spin Diffusion Measurements: Spin Echoes in the Presence of Time-Dependent Field Gradient. *J. of Chemical Physics* 1965; **42**, 288-292.

Appendices/Bibliography:

1. Dyke JP, Lauto A, Schneider E, Matei C, Borja J, Mao X, Shungu DC, Jakubowski AA, Lis E, and Ballon D. Homogeneous Water-Lipid Phantoms with Matched T_1 and T_2 Relaxation Times for Quantitative Magnetic Resonance Imaging of Tissue Composition at 3.0 Tesla (submitted to *Magnetic Resonance in Medicine*).
2. Ballon D, Watts R, Dyke JP, Lis E, and Jakubowski AA. Rapid Three-Dimensional Whole-Body Diffusion-Weighted Echo Planar Magnetic Resonance Imaging of Metastatic Neoplasia. Abstract from the Proceedings of the International Society for Magnetic Resonance in Medicine 11th Annual Meeting (2003).

Personnel:

Douglas J Ballon, PhD	Principal Investigator
Richard Watts, PhD	Co-investigator
Jonathan Dyke, PhD	Co-investigator

**Homogeneous Water-Lipid Phantoms
with Matched T_1 and T_2 Relaxation Times for Quantitative
Magnetic Resonance Imaging of Tissue Composition at 3.0 Tesla**

J.P. Dyke¹, A. Lauto^{2,4}, E. Schneider³, C. Matei⁴, J. Borja¹, X. Mao⁷, D.C. Shungu⁷,
A.A. Jakubowski⁶, E. Lis⁵, and D. Ballon^{1,4,5}

Department of Radiology¹, Weill Medical College of Cornell University,

Box 234, 1300 York Avenue, New York, NY 10021 USA

Biomedical Engineering Department², University of New South Wales, Sydney 2056, NSW, Australia

SciTrials, LLC³, Westwood, MA 02090 USA

*Departments of Medical Physics⁴, Radiology⁵, and Medicine⁶, Memorial Sloan Kettering Cancer Center,
1275 York Avenue, New York, NY 10021 USA*

Mount Sinai School of Medicine of New York University⁷

One Gustave L. Levy Place, Box 1234, New York, NY 10029 USA

Address correspondence to:

D. Ballon, Ph.D.

Citigroup Biomedical Imaging Center

Weill Medical College of Cornell University – Box 234

1300 York Avenue, New York, NY 10021 USA

djb2001@med.cornell.edu

Phone: (212) 746-5679

FAX: (212) 746-6681

Running Title: Homogeneous T_1 and T_2 Matched Water-Lipid Phantoms

Manuscript Word Count: 4502

Abstract:

Bone marrow diseases such as leukemia, metastatic cancers, and multiple myeloma affect primarily the red marrow and often result in expansion of the cellular elements throughout the medullary compartment. Disease progression or therapeutic response can be grossly assessed using longitudinal magnetic resonance imaging studies whose contrast depends upon the water-to-lipid ratio within a given voxel. Quantitative water-lipid measurements offer a means for a more precise determination of bone marrow involvement. In order to validate measurement precision and reproducibility for quantitative imaging, a set of homogenous water-lipid phantoms are proposed for use as calibration standards.

The design of solid two-component phantoms for MR imaging is presented which allows for matching of both spin-lattice and spin-spin water and methylene lipid relaxation times. Water in agarose gel and lipid phantoms with high spatial homogeneity, temporal stability, and controllable water fractions ranging from 0 to 1.0 in 0.1 increments were achieved. Composition comparisons were made using a 3-point Dixon technique as well as a stimulated echo spectroscopic method versus water fractions by weight during manufacture. Less than 5% spatial composition variation and 10% spatial variation in T_1 and T_2 were observed.

Word Count: 186

Key Words: Magnetic Resonance, Dixon, Spectroscopy, Phantoms

Introduction:

Biological magnetic resonance (MR) signals *in vivo* are known to predominantly arise from the proton spins present in water and lipids. The differential excitation, suppression, or separation of these signals has been useful for clinical and research applications, including bone marrow disease (1,2,3). However, perfect water-lipid differentiation is often beyond the capability of current scanning technology. More quantitative MR imaging or spectroscopic techniques could benefit from the use of phantoms which would serve as calibration standards for the water and fat composition of the tissue and help avoid misinterpretation of incompletely excited, suppressed or separated water or lipid signals.

Multiple phantoms that mimic tissue composition have been proposed over the past several years. One set of phantoms was comprised of a suspension of unsaturated lipids in water (4). Hilaire *et al.* used methylene chloride and partially hydrogenated soybean oil phantoms to measure the lipid component in the bone marrow (5). Other phantoms were made of a polyurethane mesh immersed in vegetable oil or a mixture of water gel with unsaturated and saturated lipids (6,7,8). Schick *et. al.* created liquid emulsion phantoms composed of 0.1%, 1% and 10% ten carbon chain length fatty acids. Lecithin was used to stabilize these suspensions (9). Homogeneous emulsion phantoms were prepared by Ruan *et al.* using Crisco, TWEEN-40, CuSO₄ and water (10). These emulsions spanned the entire compositional range, had a minimum of a 7 day shelf life, and were manufactured prior to each use.

Techniques for relative or absolute quantification of tissue composition using magnetic resonance imaging based water-lipid separation have been developed as a non-invasive means of longitudinally monitoring therapy. Two-point (2PD) and three-point (3PD) Dixon techniques (2,3,11,12,13) for water-fat separation have been used to measure the cellularity in the bone marrow of patients with leukemia (12,14,15,16,17) as well as to follow enzymatic therapy in patients with Gauchers' disease (13,18,19). Proton MR spectroscopy has also been used for the characterization of bone marrow disease (20,21,22). These methods assume that the water signal fraction is approximately equal to the hematopoietic cellular fraction in the bone marrow with respect to the fat content (5,16,20,22). Quantitative water-lipid MR techniques have also been used to monitor

changes in liver lipid content (23,24,25), muscle lipid content and distribution (9) as well as to assess breast tissue composition (26,27,28).

In this paper, a technique is presented for the fabrication of stable, homogeneous, water-lipid phantoms over the full range of relative water-to-lipid fractions. The approach is both simple and inexpensive to implement. The phantoms were designed to have the same T_1 and T_2 values for both the water and lipid components to eliminate the systematic error in the calculation of water-to-lipid fractions caused by use of finite MR measurement parameters such as echo time and pulse repetition time. The manufacturing methods, the T_1 and T_2 measurements, as well as the measured water fractions (W_f) versus those determined by weight are presented.

Materials and Methods:

Phantom Preparation

A primary feature of the phantom design was to reduce the hydrophobic reaction between water and lipids by containing the water in an agarose gel. Furthermore, it was found that by varying the concentration of agarose from 1.0 wt% to 5.0 wt% it was possible to match the T_2 value of water to that of methylene lipid. Finally, variable concentrations of Gd-DTPA (Magnevist, Berlex Labs, Wayne, NJ) were diluted in distilled water before preparation of the gel to shorten the gel T_1 and match it with the lipid T_1 (29). The T_2 values of the doped agarose gels were also measured to assess the T_2 variation due to Gd-DTPA concentration. When the concentrations of agarose and Gd-DTPA were determined such that the T_1 and T_2 values of water and lipid were matched, phantoms were constructed over the entire range of water-to-lipid percentages in 10% increments. The water-to-lipid fractions as measured by MRI were then compared to the prepared fractions as measured by weight.

Lard (Manteca, Goya of New Jersey, Secaucus, NJ) was used as the lipid compound of choice because it approximated the spectral widths and peaks observed in-vivo better than vegetable compounds. The lard complies with the standard composition set by the U.S. Department of Agriculture (30). The lard is a solid at room temperature, but easily melted using a hotplate-stirrer. Lecithin (Sunrise Health Products, Brookfield, CT) was chosen as an inexpensive and accessible emulsifying agent. Lecithin was added directly to the melted lard at a 2% fraction by weight. The mixture was continually stirred until completely dissolved.

Low melting point agarose (A9414 Agarose, SIGMA-Aldrich Corp., St. Louis, MO) and distilled water were used to create the water component of the phantoms. Enough water for a full set of phantoms and 0.6 mM of Gd-DTPA (Magnevist (938 g/mole), Berlex Labs, Wayne, NJ) was heated to boiling and a 2% fraction of agarose powder by weight of water was slowly added while continuously stirring to avoid clumping of the powder. Once mixed, the temperature of the water-agarose mixture was reduced to approximately 70 °C and placed with the lipid mixture on the same hotplate.

The desired quantity of lipid-lecithin mixture by weight was then poured into a separate beaker. An unheated magnetic stirrer was added to the beaker and the desired amount of water-agarose also weighed and slowly added while quickly stirring to achieve the desired percent water fraction. The combined mixture was removed from the stirrer when almost set, poured into a 30 ml vial and allowed to cool to room temperature.

MR Measurements

All MR image data were acquired on a 3.0 Tesla GE MRI scanner (GE Medical Systems, Milwaukee, WI) using a transmit/receive head coil. Water fractions for the entire phantom set (Figure 1) were obtained using a 3-point Dixon (3PD) (11,16) spin echo acquisition. Typical 3PD acquisition parameters were TE = 17 ms, TR = 4000 ms, matrix = 256 x 128, FOV = 24 cm and a 10 mm thick slice. T₂ measurements were performed using a multi-echo 3PD acquisition with echo times of 17, 34, 51, and 68 ms. T₁ values were estimated using a single echo 3PD acquisition and varying the pulse repetition times as in a saturation recovery method, with TR=100, 250, 500, 750, 1000, 1500, 2000 and 4000 ms.

In addition, relaxation times and water fractions were verified using a single voxel STimulated Echo Acquisition Mode (STEAM) spectroscopy sequence (PROBE-S). The vials were individually positioned in a beaker of water in the center of the standard head coil. Localized voxel shimming was performed to achieve the sharpest line width and maximum signal within the phantom. Data were acquired with TR = 4000 ms, TE = 17 ms, 2048 data points and a sweep width of 5000 Hz. Since the signal-to-noise ratios were typically of order 100:1 per excitation, only a single excitation was acquired and used for fitting.

Image Analysis

The 3PD data were transferred to a Pentium-IV IBM PC for computation of W_f using software (16) written in IDL (Research Systems Inc/Kodak, Boulder, CO). The water fraction was calculated on a voxel-by-voxel basis from the results of the Dixon decomposition as:

$$W_f(x,y) = W(x,y) / (W(x,y) + \rho F(x,y)) \quad [1]$$

The coefficient $\rho=1.1$ is a correction for the relative mass density of water versus lipid (27). The phase wraparound problem inherent in producing separate water ($W(x,y)$) and lipid ($F(x,y)$) images and image misalignment due to the chemical shift difference between the water and methylene lipid resonances were overcome using a previously published iterative algorithm (28). After regions of interest (ROI's) were selected from the W_f images, the mean and standard deviation of the signal intensities were used to assess phantom composition and spatial uniformity. T_1 and T_2 values were extracted from the water and lipid images produced from the 3-Point Dixon acquisitions. ROI's were chosen on the resulting parametric images to produce histograms of the relaxation values within the region. The histograms were fit with a Gaussian distribution and the mean of the distribution was extracted. Histograms that resulted in a bi-modal distribution were assigned a mean value using standard methods.

Spectral Analysis

Single voxel spectra were transferred from the 3.0 Tesla GE MRI to an SGI Octane workstation for analysis using XsOsNMR software (developed by X. Mao and D.C. Shungu, Mount Sinai School of Medicine, NY, NY). Data was converted from the GE format to XsOs format and Fast Fourier Transformed (FFT) after applying 2 Hz exponential filtering. Spectra were zoomed between 0.0 and 6.0 ppm and manually phased. Peak picking was performed manually on the water resonance, and 4 lipid resonances were identified as: (1-olefinic, C-H=C-H, 5.18 ppm), (2-(CH₂)' 1.93 ppm), (3-methyl, (CH₂)_n, 1.15 ppm), (4-methylene, CH₃, 0.76 ppm) (31,32). Here (CH₂)' refers to a broad resonance consisting of several components with CH₂ groups bound to a neighbouring unsaturated carbon atom. Frequency domain fitting was performed using a Levenberg-Marquardt algorithm and a Lorentzian function optimizing frequency, amplitude and width. Peak areas were calculated and used for comparison of water fractions to those obtained using the 3PD method.

Results:

Effect of Agarose Concentration on T_2 Value

An increase in the dry weight percent of the agarose gel from 1.0 wt% to 5.0 wt% was compared with the T_2 values of water and lipid in a phantom containing 50% water and 50% lard by weight. The addition of agarose caused a systematic decrease of the water T_2 value (Figure 2) (33,34). The lipid T_2 was invariant with changes in agarose concentration, with a mean value of 28.0 ± 1.6 ms. The water and lipid T_2 curves crossed at an agarose gel concentration of approximately 2.0 wt% which was used in subsequent phantoms to provide matched T_2 values.

Effect of Gd-DTPA on T_1 and T_2 Values

The T_1 values of water in a 2.0 wt% agarose gel phantom containing 50% water and 50% lard by weight systematically decreased with increasing concentration of Gd-DTPA from 0 to 1.4 mM (Figure 3a). The spin-lattice relaxivity of water due to Magnevist was calculated to be 5.58 /mM /sec at 3.0 T ($R^2 = 0.99$). The crossing of the water and lipid T_1 curves occurred at an approximate concentration of 0.6 mM Gd-DTPA in the 2.0 wt% agarose gel. The Gd-DTPA appeared to remain stable at 100°C and retained its relaxivity characteristics within the gel and phantoms (29). No effect on phantom T_2 values for water or lipid was found as a function of Gd-DTPA concentration (Figure 3b). The water component of the phantom yielded $T_2 = 30.1 \pm 4.4$ ms, which matched that of the lipid component at 29.8 ± 2.0 ms.

Water-Lipid Phantoms

A set of water/lipid phantoms was prepared using 0.6 mM Gd-DTPA doped agarose gel at 2.0 wt% with the addition of 2.0 wt% lecithin. Using the 3PD technique, the measured W_f and the water fraction by weight displayed a noticeable variance from linear behaviour with respect to percentages by weight (Figure 4). This was not observed for the measurements made using magnetic resonance spectroscopy. A typical spectrum from a phantom consisting of 50% water and 50% lard by weight is shown in Figure 5. The phantoms were determined to be spatially homogeneous to within a water fraction of approximately 5%. The T_1 values of the water and lipid components were 259.8 ± 23.8 ms vs. 275.0 ± 11.0 ms ($n=10$) as shown in Figure 6a. Water T_2 values (30.7 ± 3.4 ms, $n=10$) were also reasonably well matched to those of the lipid (26.3 ± 1.7 ms, $n=10$) as shown in

Figure 6b, although there was some spatial variation in the relaxation times across different samples.

Discussion:

A question of fundamental relevance to this work is how well a magnetic resonance measurement can approximate the water-to-lipid content as measured by weight. Assuming a density for water of 1.0 g/cm^3 at room temperature yields 0.110 mole/cm^3 of protons. Using a lipid density of 0.9 g/cm^3 and a representative triacylglycerol molecular weight of 860 g/mole as a model for the lipid component (35) of the phantoms yields 0.109 mole/cm^3 of protons bound in fat. The two numbers are equal to within approximately 1%, and are the basis of the argument that magnetic resonance is useful for measuring water-to-lipid ratios in the phantoms and in tissue. In practice, there are however several other factors which must be accounted for to ensure the accuracy of the magnetic resonance measurement (16). The most important of these are the correction for the differential relaxation time of water and lipid protons and the fact that the lipid spectrum has multiple resonances. In this regard Gd-DTPA doping achieved matched T_1 values for the water and lipid components. Similarly, the T_2 value of water in the gel was made comparable to the T_2 of the lipids by varying the agarose concentration, in agreement with the findings of prior authors (33,34).

In tissue, the relaxation times themselves are a complex average over different molecular environments and compartments. For the phantoms, the problem is simplified, but still involves an implicit average over the relaxation times of methylene and methyl resonances for the lipid component, and an average over the olefinic proton of lipid and the water resonances for the water component at lower water concentrations.

The 3PD imaging approach allows for high resolution images of the water and lipid components of a sample. However, a limitation of the method is the fact that only two distinct frequencies are easily accounted for in the water fraction calculation, while other resonances have a phase that is modulated by a cosine function of resonance offset (5,11,31). The two chosen frequencies were the center of the water resonance and the center of the methylene lipid resonances for this work. Magnetic resonance spectroscopy does not suffer from this limitation and was used to allow calculations of the water fraction by considering individual resonances. This provided an independent check on the accuracy of the 3PD

method. The deviation from linear behavior for 3PD in Figure 4 can be explained by calculating the water fraction using all resonances observed in the spectroscopic measurement as

$$W_f = W / (W + \rho[O + (CH_2)' + (CH_2)_n + CH_3]), \quad [2]$$

where the lipid component has been resolved into olefinic (O), $(CH_2)'$, $(CH_2)_n$ and CH_3 resonances. In Eq. [2] the olefinic lipid resonance has been appropriately grouped with the other lipid contributions. Using this method a linear relationship was obtained versus measurement by weight with $R^2 = 0.99$. Moreover, calculation of the water fraction using only the water and $(CH_2)_n$ resonance yielded a curve that was in close agreement with 3PD method, as expected.

The preparation of solid water-lipid phantoms presented the challenging task of homogeneously mixing hydrophobic molecules with water. Ideal phantoms should be stable, without lipid aggregation due to hydrophobic forces and without growth of mold. These obstacles were overcome by the addition of a low concentration emulsifying agent. This allowed the manufacture of amalgamated phantoms with a good spatial homogeneity. The phantoms did not require careful handling during their transport and use. In general, construction of the phantoms using large single batches of water-agarose and lard-lecithin versus individual batches for each vial were preferable as they reduced relative measurement errors that tend to accumulate in measuring the constituent ingredients.

Conclusions:

A method has been presented for the construction of water-lipid phantoms for MR imaging and spectroscopy with matched spin-lattice and spin-spin relaxation times. The phantoms described herein are stable and homogeneous, and span the entire range of water-to-lipid ratios. The techniques afford less than 5% spatial variation in composition and 10% in relaxation times.

T_1 and T_2 matching was achieved using a 0.6 mM gadolinium solution combined with agarose powder to form a doped 2.0 wt% agarose gel with the addition of 2.0 wt% lecithin to

the lard as an emulsifying agent. The mean T_1 and T_2 values of the gel and lipid components at 3 Tesla were as follows: $T_{1\text{Water}} = 259.8 \pm 23.8$ ms; $T_{1\text{Lipid}} = 275.0 \pm 11.0$ ms; $T_{2\text{Water}} = 30.7 \pm 3.4$ ms; $T_{2\text{Lipid}} = 26.3 \pm 1.7$ ms.

Acknowledgements:

This work was supported in part by grants from the National Heart, Lung and Blood Institute (R01EB002070), the Susan G. Komen Breast Cancer Foundation, Pfizer, Inc, and the United States Army Medical Research and Materiel Command (BC995795).

Figure Captions:

- Figure 1:** Proton density 3PD water-only (A), lipid-only (B), and water fraction (C) images are shown from a set of water-lipid phantoms with water fractions ranging from 0 to 1.0 in increments of 0.1.
- Figure 2:** T_2 values for both water and lipid in a phantom containing 50% water and 50% lard by weight, with 2.0 wt% lecithin added as an emulsifying agent plotted as a function of dry weight percent agarose powder.
- Figure 3:** (A) T_1 values for water and lipid in a phantom containing 50% water and 50% lard by weight, 2.0 wt% agarose gel, and 2.0 wt% lecithin plotted as a function of Gd-DTPA concentration. (B) T_2 values for water and lipid in a phantom containing 50% water and 50% lard by weight, 2.0 wt% agarose gel, and 2.0 wt% lecithin plotted as a function of Gd-DTPA concentration.
- Figure 4:** The measured water fraction as determined by magnetic resonance imaging and spectroscopy compared to that determined by weight.
- Figure 5:** The STEAM spectral acquisition for the 50% water and 50% lard phantom is shown with the composite spectral fit to the original data (A) the individual resonances comprising the fit (B) and the residual (C). Individual resonances are: olefinic, H-C=C-H , 5.18 ppm; $(\text{CH}_2)'$ (see text), 1.93 ppm; methyl, $(\text{CH}_2)_n$, 1.15 ppm; and methylene, CH_3 , 0.76 ppm.
- Figure 6:** (A) T_1 and (B) T_2 relaxation times for water and lipid components of the full set of water fraction calibration phantoms.

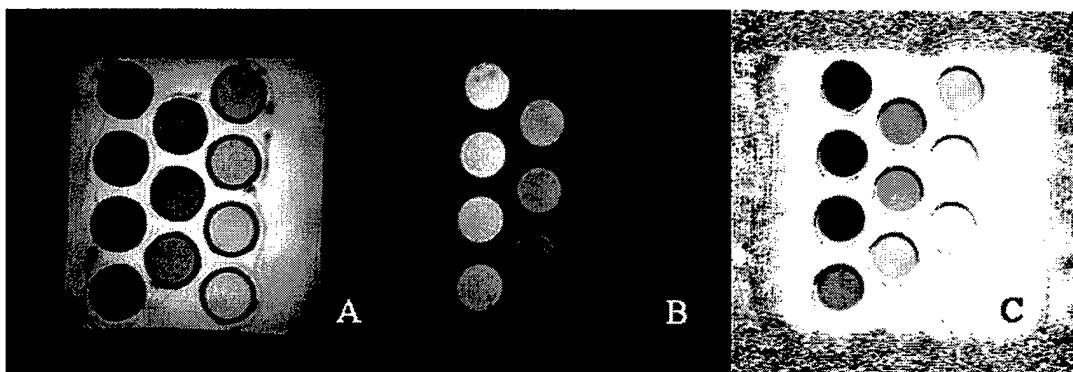


Figure 1: Proton density 3PD water-only (A), lipid-only (B), and water fraction (C) images are shown from a set of water-lipid phantoms with water fractions ranging from 0 to 1.0 in increments of 0.1.

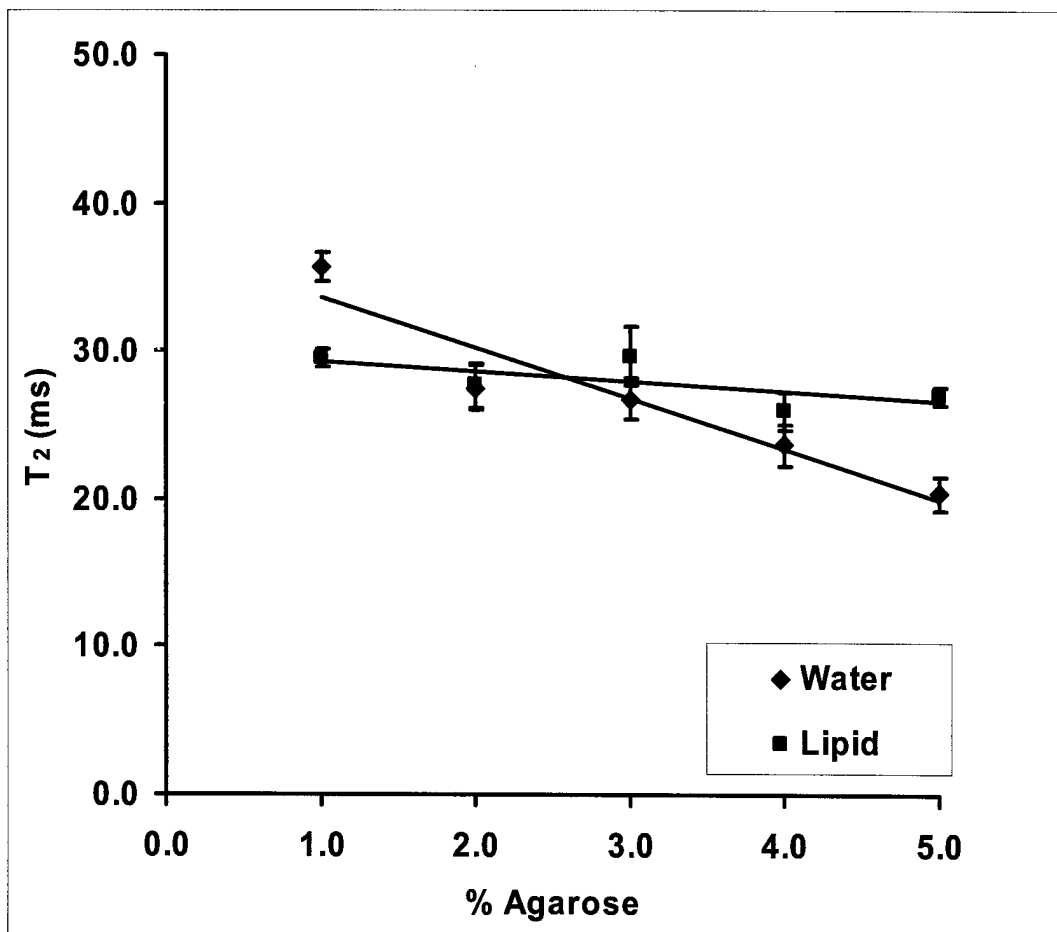
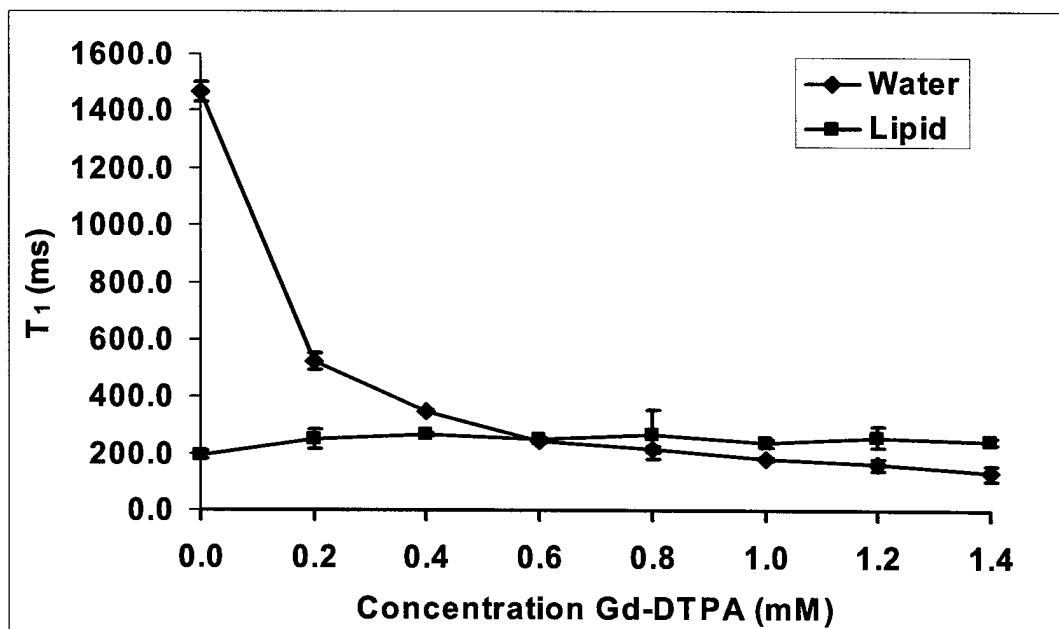
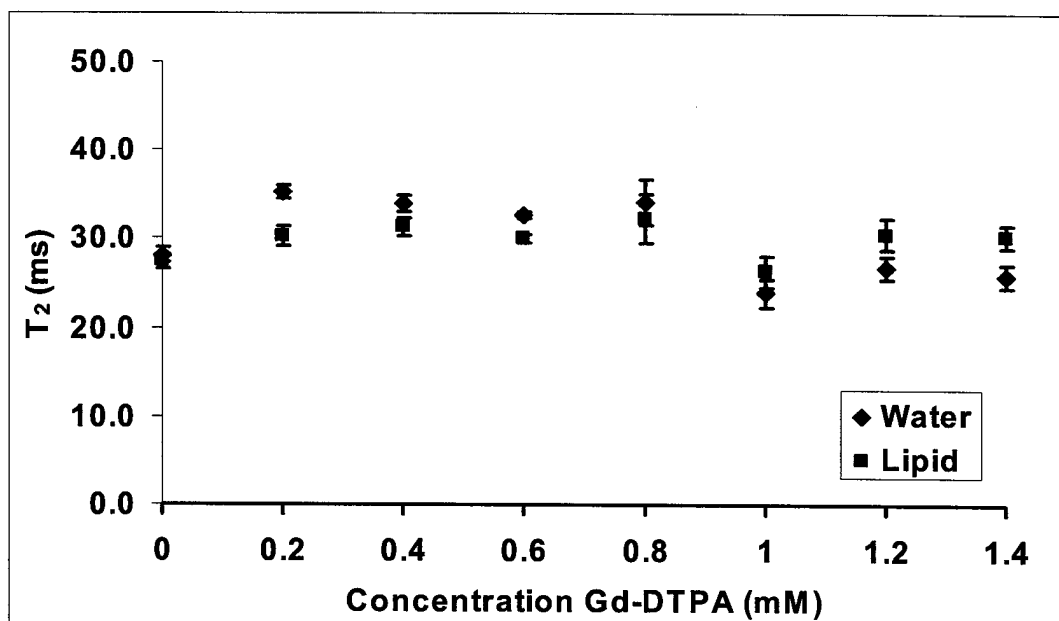


Figure 2: T₂ values for both water and lipid in a phantom containing 50% water and 50% lard by weight, with 2.0 wt% lecithin added as an emulsifying agent plotted as a function of dry weight percent agarose powder.



(A)



(B)

Figure 3: (A) T_1 values for water and lipid in a phantom containing 50% water and 50% lard by weight, 2.0 wt% agarose gel, and 2.0 wt% lecithin plotted as a function of Gd-DTPA concentration. (B) T_2 values for water and lipid in a phantom containing 50% water and 50% lard by weight, 2.0 wt% agarose gel, and 2.0 wt% lecithin plotted as a function of Gd-DTPA concentration.

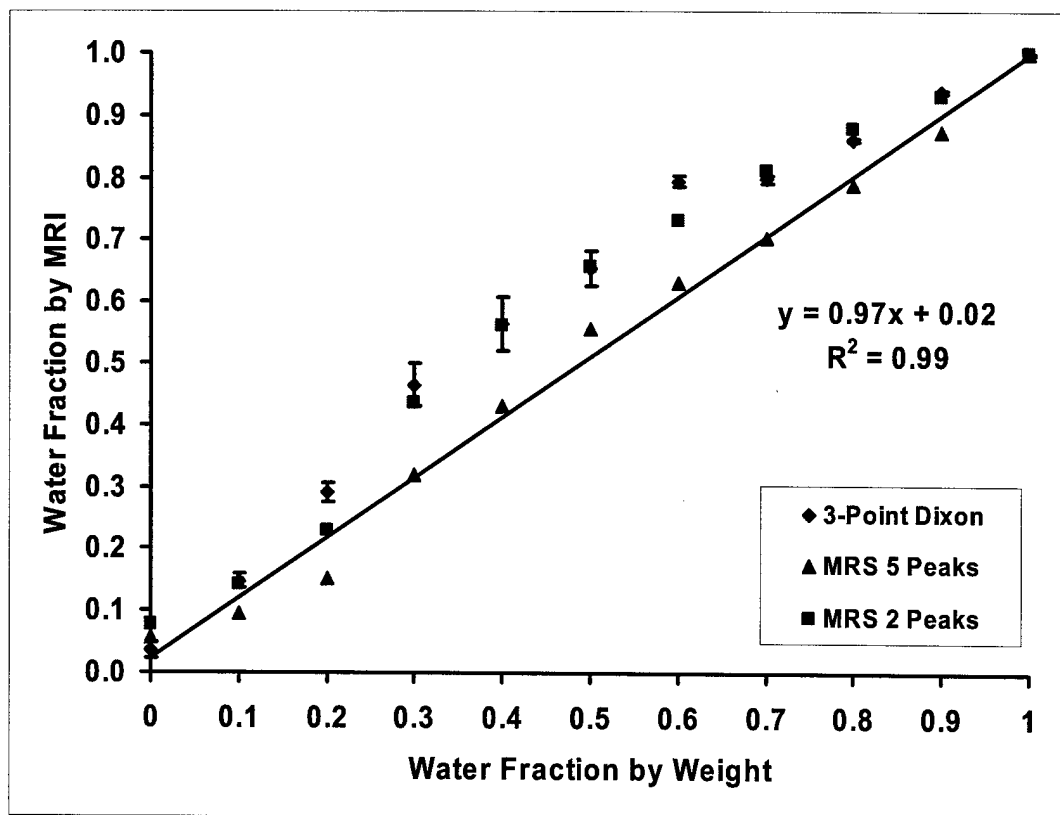


Figure 4: The measured water fraction as determined by magnetic resonance imaging and spectroscopy compared to that determined by weight.

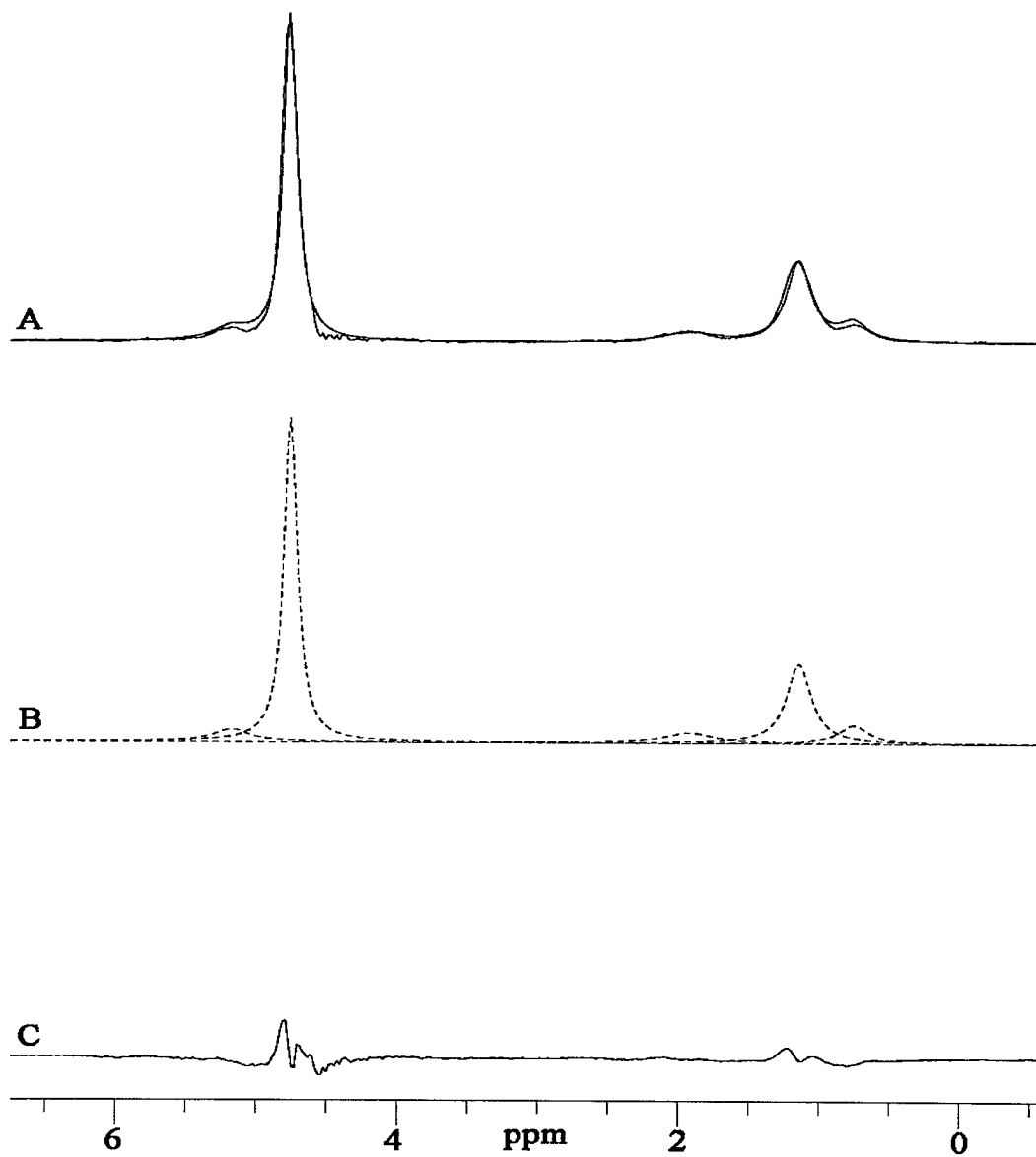
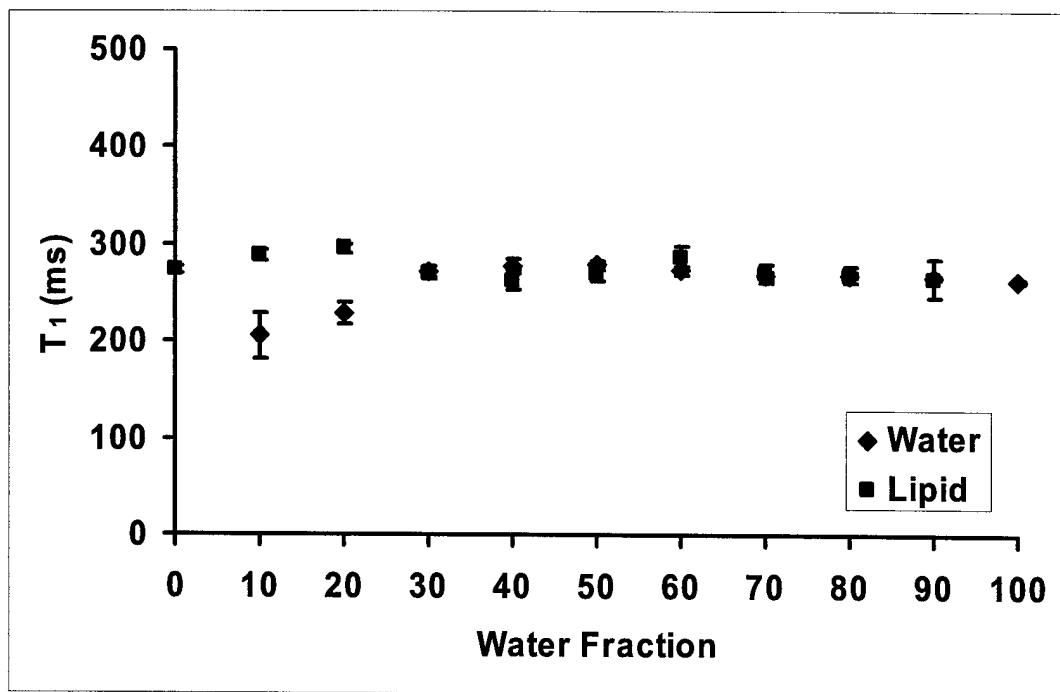
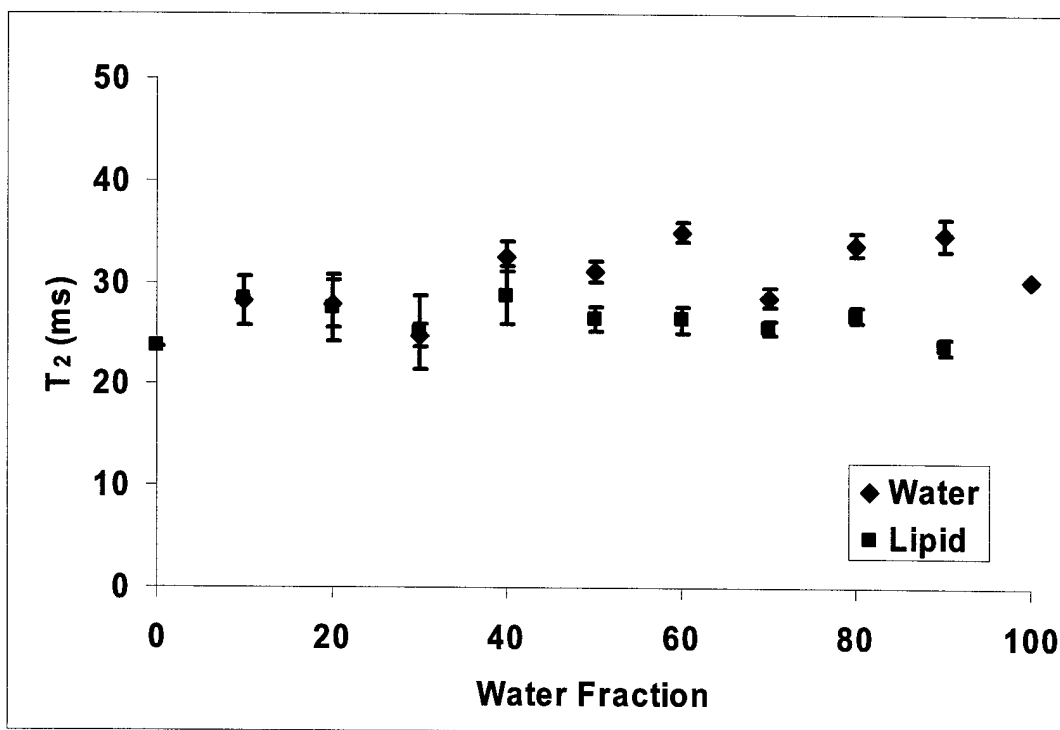


Figure 5: The STEAM spectral acquisition for the 50% water and 50% lard phantom is shown with the composite spectral fit to the original data (A) the individual resonances comprising the fit (B) and the residual (C). Individual resonances are: olefinic, H-C=C-H , 5.18 ppm; $(\text{CH}_2)'$ (see text), 1.93 ppm; methyl, $(\text{CH}_2)_n$, 1.15 ppm; and methylene, CH_3 , 0.76 ppm.



(A)



(B)

Figure 6: (A) T₁ and (B) T₂ relaxation times for water and lipid components of the full set of water fraction calibration phantoms.

References:

- 1 Haacke EM, Patrick JL, Lenz GW, Parrish T. The separation of water and lipid components in the presence of field inhomogeneities. *Rev Magn Reson Med* 1986;1(2):123-154.
- 2 Dixon WT. Simple proton spectroscopic imaging. *Radiology* 1984;153(1):189-94.
- 3 Ma J, Wehrli FW, Song HK, Hwang SN. A single-scan imaging technique for measurement of the relative concentrations of fat and water protons and their transverse relaxation times. *J Magn Reson* 1997;125(1):92-101.
- 4 D'Souza WD, Madsen EL, Unal O, Vigen KK, Frank GR, Thomadsen BR. Tissue Mimicking Materials for a Multi-Imaging Modality Prostate Phantom. *Med Phys* 2001;28:688-700.
- 5 Hilaire L, Wehrli FW, Song HK. High Speed Spectroscopic Imaging for Cancellous Bone Marrow R2* Mapping and Lipid Quantification. *Magn Reson Imaging* 2000;18:777-786.
- 6 McDannold N, Hynynen K, Oshio K, Mulkern RV. Temperature monitoring with line scan echo planar spectroscopic imaging. *Med Phys* 2001;28:346-55.
- 7 Wagnieres G, Cheng S, Zellweger M, Utke N, Braichotte D, Ballini JP, Van Den Berg H. An Optical Phantom with Tissue Like Properties in the Visible for use in PDT and Fluorescence Spectroscopy. *Phys Med Biol* 1997;42:1415-1426.
- 8 Mitchell DG, Stolpen AS, Siegelman ES, Bolinger L, Outwater EK. Fatty tissue on opposed-phase MR images: paradoxical suppression of signal intensity by paramagnetic contrast agents. *Radiology* 1996;198:351-357.
- 9 Schick F, Machann J, Brechtel K, Strempfer A, et al. MRI of muscular fat. *Magn Reson Med* 2002;47(4):720-727.
- 10 Ruan R, Chang K, Chen P, Fulcher R, Bastian E. A magnetic resonance imaging technique for quantitative mapping of moisture and fat in a cheese block. *J Dairy Science* 1998;80:9-15.
- 11 Glover GH, Schneider E. Three-Point Dixon Technique for True Water/Fat Decomposition with B₀ Inhomogeneity Correction. *Magn Reson Med* 1991;18:371-383.
- 12 Guckel F, Brix G, Semmler W, Zuna I, Knauf W, Ho AD, van Kaick G. Systemic bone marrow disorders: characterisation with proton chemical shift imaging. *J Comput Assist Tomogr* 1990;14:633-642.
- 13 Maas M, Hollak C, Aerts J, Stoker J, Den Heeten J. Quantification of Skeletal Involvement in Adults with Type 1 Gaucher's Disease: Fat Fraction Measured by Dixon Quantitative Chemical Shift Imaging as a Valid Parameter. *Am J Roentgen* 2002;179:961-965.

-
- 14 Rosen BR, Fleming DM, Kushner DC, et al. Hematologic bone marrow disorders: quantitative chemical shift MR imaging. *Radiology* 1988;169:799-804.
- 15 Gerard EL, Ferry JA, Amrein PC, Harmon DC, McKinstry RC, Hoppel BE, Rosen BR. Compositional changes in vertebral bone marrow during treatment for acute leukemia: assessment with quantitative chemical shift imaging. *Radiology* 1992;183:39-46.
- 16 Ballon D, Jakubowski AA, Tulipano PK, Graham MC, Schneider E, Aghazadeh B, Chen QS, Koutcher JA. Quantitative assessment of bone marrow hematopoiesis using parametric magnetic resonance imaging. *Magn Reson Med* 1998;39(5):789-800.
- 17 Maas M, Akkerman EM, Venema HW, Stoker J, den Heeten GJ. Dixon Quantitative Chemical Shift MRI for Bone Marrow Evaluation in the Lumbar Spine: A Reproducibility Study in Healthy Volunteers. *J Comput Assist Tomogr* 2001;25(5):691-697.
- 18 Mankin HJ, Rosenthal DI, Xavier R. Gaucher Disease: New Approaches to an Ancient Disease. *J Bone Joint Surg Am* 2001;83-A(5):748-762.
- 19 Hollak C, Maas M, Akkerman E, den Heeten A, Aerts H. Dixon Quantitative Chemical Shift Imaging Is a Sensitive Tool for the Evaluation of Bone Marrow Responses to Individualized Doses of Enzyme Supplementation Therapy in Type 1 Gaucher Disease. *Blood Cells Mol Dis* 2001;27(6):1005-1012.
- 20 Ballon D, Jakubowski AA, Gabrilove J, Graham MC, Zakowski M, Sheridan C, Koutcher JA. In vivo measurements of bone marrow cellularity using volume-localized proton NMR spectroscopy. *Magn Reson Med* 1991;19(1):85-95.
- 21 Buxton RB, Wismer GL, Brady TJ, Rosen, BL. Quantitative proton chemical shift imaging. *Magn Reson Med* 1986;3:881-900.
- 22 Kugel H, Jung C, Schulte O, Heindel W. Age- and Sex-Specific Differences in the ^1H Spectrum of Vertebral Bone Marrow. *J. Magn. Reson. Imaging* 2001;13:263-268.
- 23 Fishbein MH, Miner M, Mogren C, Chalekson J. The spectrum of fatty liver in obese children and the relationship of serum aminotransferases to severity of steatosis. *J Pediatr Gastroenterol Nutr.* 2003;36(1):54-61.
- 24 Fishbein MH, Stevens WR. Rapid MRI using a modified Dixon technique: a non-invasive and effective method for detection and monitoring of fatty metamorphosis of the liver. *Pediatr Radiol.* 2001;31(11):806-9.
- 25 Levenson H, Greensite F, Hoefs J, Friloux L, Applegate G, Silva E, Kanel G, Buxton R. Fatty infiltration of the liver: quantification with phase-contrast MR imaging at 1.5 T vs biopsy. *Am J Roentgenol.* 1991;156(2):307-12.

-
- 26 Graham SJ, and Bronskill MJ. MR Measurement of Relative Water Content and Multicompartment T2 Relaxation in Human Breast. *Magn. Reson. Med.* 1996;35, 706-715.
- 27 Graham SJ, Stanchev PL, Lloyd-Smith JOA, Bronskill MJ, and Plewes DB. Changes in fibroglandular volume and water content of breast tissue during the menstrual cycle observed by MR imaging at 1.5 Tesla. *J Magn Reson Imaging* 1995;5:695-701.
- 28 Chen Q, Schneider E, Aghazadeh B, Weinhaus MS, Humm J, Ballon D. An automated iterative algorithm for water and fat decomposition in three-point Dixon magnetic resonance imaging. *Med Phys.* 1999;26(11):2341-2347.
- 29 Gd-DTPA (Magnevist, Berlex Labs, Wayne, NJ). Package Insert.
- 30 US Department of Agriculture, Agricultural Research Service. Nutrient Database for Standard Reference (1999). <http://www.nal.usda.gov/fnic/foodcomp>
- 31 Brix G, Heiland S, Bellemann ME, Koch T, Lorenz W. MR imaging of fat-containing tissues valuation of two quantitative imaging techniques in comparison with localized proton spectroscopy. *Magn Reson Imaging* 1993;11:997-991.
- 32 Kuroda K, Oshio K, Mulkern RV, Jolesz FA. Optimization of chemical shift selective suppression of fat. *Magn Reson Med.* 1998;40(4):505-10.
- 33 Mitchell MD, Kundel HL, Axel L, Joseph PM. Agarose as a tissue equivalent phantom material for NMR imaging. *Magn Reson Imaging* 1986;4(3):263-6.
- 34 Rice JR, Milbrandt RH, Madsen EL, Frank GR, et al. Anthropomorphic 1H MRS head phantom. *Med Phys* 1998;25(7 Pt 1):1145-56.
- 35 Stryer L. *Biochemistry*, 3rd Edition. Chapter 20. New York: W Freeman and Company; 1988. 1089 p.

Rapid Three-Dimensional Whole-Body Diffusion-Weighted Echo Planar Magnetic Resonance Imaging of Metastatic Neoplasia

D. Ballon¹, R. Watts¹, J. P. Dyke¹, E. Lis², A. A. Jakubowski²

¹Weill Cornell Medical College, New York, NY, United States, ²Memorial Sloan-Kettering Cancer Center, New York, NY, United States

Synopsis

A technique is presented for whole-body evaluation of metastatic neoplasia in bone marrow at a spatial resolution of 56 mm³ in under 15 minutes without contrast agents using diffusion-weighted echo planar magnetic resonance imaging. The segmentation of metastatic disease relative to the strong overlying signals from water in other anatomy was achieved through the use of strong T₂ and diffusion weighting combined with high quality lipid suppression. Three-dimensional projection displays were developed for image interpretation. The methods have potential application to the evaluation of tumor burden in hematologic and metastatic disease as well as to therapeutic monitoring.

Introduction

The assessment of hematologic disease in humans is generally achieved through analysis of a bone marrow biopsy or aspirate from either the iliac crests or sternum combined with examination of the peripheral blood. In cases of distant focal bone marrow metastases from a known primary tumor, direct assessment of the metastatic phenotype is even more difficult since the tumors are often inaccessible to all but a surgical biopsy. While bone scans and PET afford a means to examine bone/bone marrow, these techniques require injected radiotracers for generation of image contrast and in the case of the bone scan are an indirect measure of tumor activity.

Materials and Methods

All image data was acquired on a 1.5 Tesla MRI system (GE Medical Systems, Milwaukee WI). A single-shot EPI sequence was used to acquire data from up to 8 stations of 30 contiguous axial slices covering the entire body (~1.8m) with 4 slices of overlap between the stations, a slice thickness of 7 mm with a 36X36 cm² field-of-view at a matrix size of 128X128 using a TR/TE of 10 s/100 ms (1,2). Diffusion weighting was applied at b=1000 s/mm² and the total scan time per station was 40 s. The diffusion trace images obtained for all the stations were stored in a single three-dimensional array and the data were typically displayed in a rotating format with each frame represented by a maximum intensity projection image. For assessment of the methods, a total of 17 scans were performed on 14 subjects, including bone marrow donors (n=4), and patients with hematologic disease (n=7) or breast cancer metastatic to bone marrow (n=3).

Results

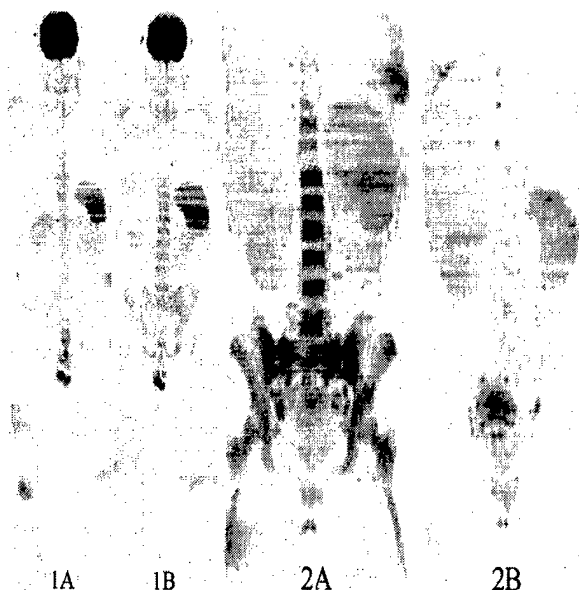
An example of a maximum intensity projection image from a whole-body dataset is presented in Figure 1. The data were taken from a normal adult volunteer receiving granulocyte colony stimulating factor (G-CSF) prior to stem cell harvest for donation to a sibling with acute myelogenous leukemia (AML). Figure 1A was obtained at baseline and Figure 1B on Day 5 of G-CSF administration. Most apparent are the changes in bone marrow intensity after G-CSF-administration, which were consistent with the increase in water T₂ value, while at the same time reflecting an increase in bone marrow cellularity from 44% to 59%. No significant change in the apparent diffusion coefficient was observed. The size of the spleen increased, which has been reported in some patients receiving G-CSF. Figure 2A presents a patient with AML prior to a course of ablative therapy. The axial skeleton and proximal femora exhibit a strong signal intensity consistent with leukemic infiltration, and the spleen is enlarged. This patient originally presented with a chloroma in the left breast, which is visible above the spleen. The patient was studied again after achieving a complete remission following therapy (Figure 2B). The signal from the bone marrow and spleen is almost completely absent.

Discussion

An important aspect of the technique was the utilization of simultaneous T₂ and diffusion weighting combined with spatial-spectral excitation of the water resonance to obtain the image contrast presented in the figures. The diffusion weighting tended to filter out extracellular fluid such as blood, CSF and urine in the images. The strong T₂ (TE=100 ms) weighting discriminated against water arising in muscle and many other organs, and the excitation pulse provided good quality lipid suppression in most cases. The most prevalent remaining signals arose from the brain, kidneys, spleen, prostate, and testes. The fact that bone marrow lesions were visible relative to normal bone marrow was due to an increase in water T₂ (62.1 ± 6.2 ms, n=7 vs. 44.0 ± 5.7 ms, n=4) as is common in neoplasia, coupled with an increase in cellularity. Conversely, no significant change in the ADC was noted between normal and diseased bone marrow in the fourteen subjects studied. Magnetic susceptibility related image distortion was minimized through the use of axial slices grouped in multiple imaging stations, with each station centered at the magnet isocenter. Combining these multiple stations gives an effective field-of-view of 1.8 m, which is sufficient for whole-body imaging. One advantage of this method is that it is amenable to direct comparison with other whole-body imaging techniques. The methods described afford a means to rapidly evaluate metastatic neoplasia and provide a particularly convenient format for the evaluation of bone marrow metastases.

References

- 1) Pauly J, Spielman D, and Macovski A. Echo-Planar Spin-Echo and Inversion Pulses, *Magnetic Resonance in Medicine*, 1993; 29, 776-782.
- 2) Schick F, Forster J, Machann J, Kuntz R, and Claussen CD. Improved Clinical Echo-Planar MRI Using Spatial-Spectral Excitation, *J. of Magn. Res. Imag.*, 1998; 8, 960-967.



Maximum intensity projections of diffusion-weighted images (b=1000 s/mm²) from two subjects. Figure 1 - Bone marrow donor: A) pre G-CSF, B) post G-CSF, Figure 2 - AML patient: A) pre-therapy, B) in remission.